XVII IMEKO World Congress
Metrology in the 3rd Millennium
June 22–27, 2003, Dubrovnik, Croatia

LOAD DEPENDENCY OF THE MOMENT-ARM LENGTH IN THE TORQUE STANDARD MACHINE

Koji Ohgushi[1], *Takashi Ota*[1], *Kazunaga Ueda*[1],
Diedert Peschel[2] *and Thomas Bruns*[2]

[1]National Metrology Institute of Japan, AIST, Tsukuba, Japan
[2]Physikalisch-Technische Bundesanstalt, Braunschweig, Germany

Abstract – The deadweight loading dependency of the moment-arm length in the torque standard machine (TSM) at NMIJ was suspected of causing deviation in the Inter-laboratories Comparison between PTB and NMIJ. The authors attempted to re-verify the moment-arm length and to improve the uncertainty of the arm length in the TSM. Metal bands (MBs) are used for the loading point (called "Reference Line") at both ends of the arm. In an arm balancing test, displacement of the MBs in the arm length direction was measured by eddy current type non-contact sensors during deadweight loading. Additional initial weights mounted just under the MBs effectively reduced the load-dependency of the arm length from 52 ppm to 24 ppm.

Keywords: Torque, Load Dependency, Arm Length

1. INTRODUCTION

A multilateral comparison of torque standards was carried out among Physikalisch-Technische Bundesanstalt (PTB, Germany), National Institute of Metrology (NIM, China), Shanghai Marine Equipment Research Institute (SMERI, China) and National Metrology Institute of Japan (NMIJ/AIST, Japan), from October to November, 2001. The results were evaluated in the form of a bilateral comparison between each laboratory and PTB, respectively. Comparison between PTB and NMIJ was conducted within the range from 10 N·m to 1 kN·m. Calibration results of NMIJ for the torque transfer standards (combination of precise torque transducers and high-resolution strain gauge amplifiers, having rated capacities of 100, 500 and 1000 N·m) deviated about 50 to 150 ppm below from the values of PTB[1] as shown in Fig.1. The deadweight loading dependency of the moment-arm length in the torque standard machine (1 kN·m-DWTSM) at NMIJ was suspected of one of causes for the ILC deviation. The authors attempted to re-verify the moment-arm length and to improve the uncertainty of the arm length in the 1 kN·m-DWTSM of NMIJ.

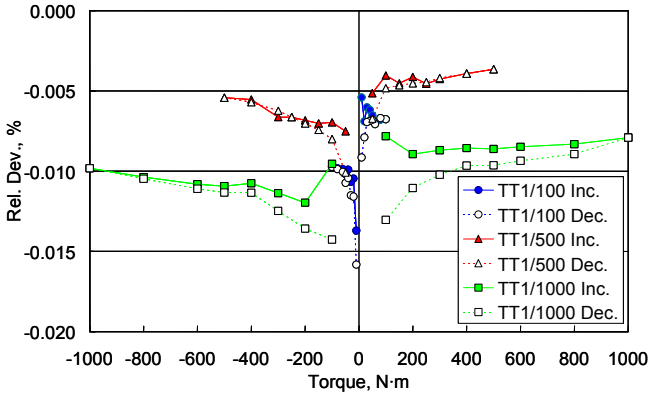

Fig. 1 Result of the ILC of torque

2. CONFIRMATION OF LOAD DEPENDENCY

2.1 Experimental procedure

An arm balancing test was carried out, in which torque transducers of small rated capacities (10 N·m and 100 N·m) were mounted on the machine and two deadweights of equal mass were loaded at both ends of the moment-arm as shown in Fig.2. Thin metal bands (MBs) are being used for the loading point (called "Reference Line") as shown in Fig.3. The re-evaluation of the arm length concerns this reference line[2].

The composition of the series of linkage weights is as follows:
· 10 N × 11 disks (5 N·m to 55 N·m),
· 20 N × 22 disks (10 N·m to 110 N·m) and
· 100 N × 22 disks (50 N·m to 1100 N·m).
Here, the nominal moment-arm length is L = 500 mm. The values of arm lengths at 20 °C measured by the Coordinate Measurement Machine (CMM) have been obtained as follows[3]:

$$L_0 = L_u + \frac{t_w}{2}, \quad (1)$$

$$L_{u(R)} = 499{,}9645 \pm 0{,}0036 \text{ mm},$$

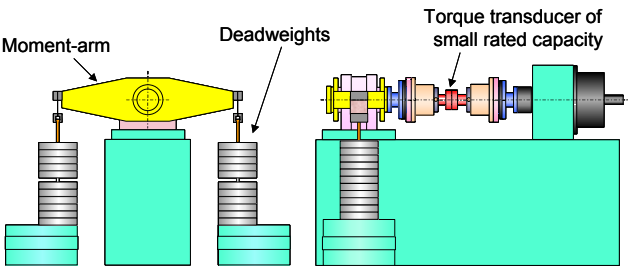

Fig. 2 Arm balancing test by 1 kN·m-DWTSM

$L_{u(L)}$ = 499,9669 ± 0,0036 mm,
$t_{w(R)}$ = 0,1009 ± 0,0010 mm,
$t_{w(L)}$ = 0,1010 ± 0,0010 mm,
$L_{0(R)}$ = 500,0149 ± 0,0049 mm and
$L_{0(L)}$ = 500,0172 ± 0,0049 mm.

(R) and (L) mean each arm length on the right side and left side. The latter values were expanded uncertainties (k = 2). If there were no dependency, $\Delta T/T = (T_{(R)}\text{-}T_{(L)})/T$ (the relative torque ratio between clockwise and counter-clockwise torques) would be constant (-5 ppm).

2.2 Result

The result of three times of measurement in the arm balancing test indicated a small average torque ratio $\Delta T/T$ of +67 ppm (small clockwise torque) at the equivalent torque of 5 N·m as shown in Fig.4. This torque deviation gradually decreased as the deadweight loading was increased, and finally saturated at +16 ppm at 1 kN·m. Since the expanded relative uncertainty of mass of each weight is less than ±5 ppm, the result clearly indicated the existence of load dependency in the arm length. In addition, the arm ratio of +16 ppm was different from the values obtained by CMM measurement (-5 ppm).

3. TORSIONAL SPRING MODEL

3.1 Principle

In order to clarify the load dependency of the arm length, a torsional spring model of MBs was proposed. This model supposes that each MB has torsional spring constant β and is holds at an angle to the vertical in the no-loading state as shown in Fig.5. As the load increases, the MBs gradually approach the vertical direction, and the arm length varies.

The lower end of the MB of length r keeps its position at x_0 and angle θ_0 from the vertical without loading. When the loading W_i by deadweight i occurs, the position and angle become x_i and θ_i. From the equilibrium of forces, the following equation is obtained:

$$\beta(\theta_0 - \theta_i) = W_i \sin\theta_i \,. \tag{2}$$

Since θ_0 and θ_i are very small, (2) can be rewritten as

$$x_i = \frac{\beta}{W_i + \beta} x_0 \,. \tag{3}$$

The torque ratio is expressed as

$$\frac{\Delta T}{T} = \frac{T_{(R)} - T_{(L)}}{T} = \frac{(L_{(R)} + x_{i(R)}) \cdot W_i - (L_{(L)} + x_{i(L)}) \cdot W_i}{L \cdot W_i} \,. \tag{4}$$

Equation (4) can be rearranged as follows provided β is the same in MBs on both the right and left sides:

$$\frac{\Delta T}{T} = C_A + C_B \frac{\beta}{W_i + \beta} \,, \tag{5}$$

where,

$$C_A = \frac{L_{(R)} - L_{(L)}}{L} \text{ and} \tag{6}$$

$$C_B = \frac{x_{0(R)} - x_{0(L)}}{L} \,. \tag{7}$$

Adopting a double logarithmic scale, (5) can be changed to a linear relationship between torque ratio and deadweight loading as follows:

$$\ln\left(\frac{\Delta T}{T} - C_A\right) = \ln(C_B\beta) - \ln(W_i + \beta) \,. \tag{8}$$

3.2 Experimental procedure

In the arm balancing test, the displacement of the MB in the arm length direction was measured by eddy current type non-contact sensors, at r = 48 mm, which was the lower position from the height of the torque measuring axis. Figure 6 shows the set up of the displacement sensors. The output voltage of the sensor is ±5 V for the clearance from 0 to 2 mm. The resolution and the expanded uncertainty are 0.1 μm and 2 μm.

The arm balancing test described in section 2.1 was conducted again, in which deadweights were loaded on both

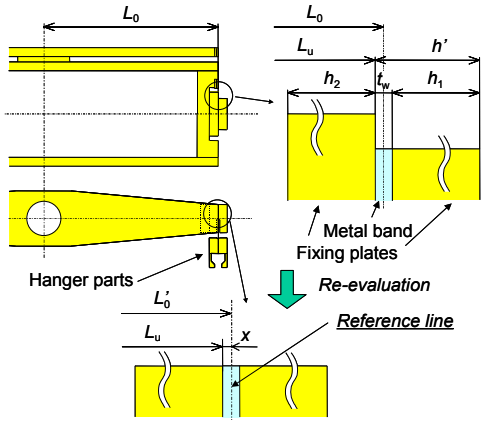

Fig. 3 Definition of dimensions in the moment-arm

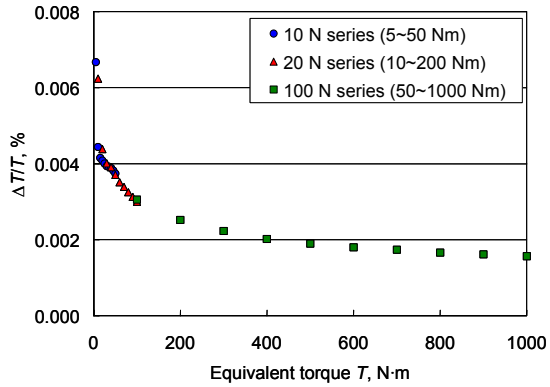

Fig. 4 Small torque ratio observed in the 1 kN·m-DWTSM

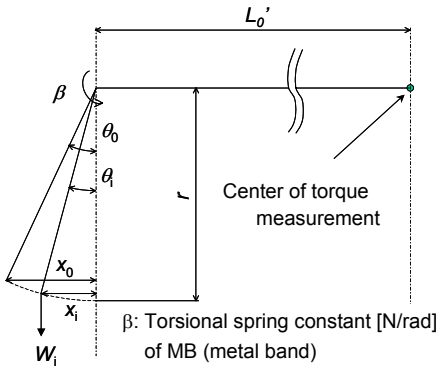

Fig. 5 Torsional spring model

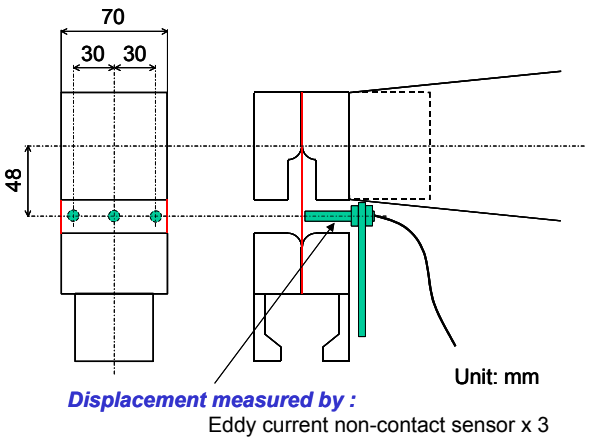

Fig. 6 Set up of the displacement measurement

sides from W = 10 N (T = 5 N·m) to 2000 N (1000 N·m). The small torque ratio from the output of the torque transducer was measured at each loading step as well as the displacement in the arm length direction. In addition, small weights were loaded on the linkage weight on the opposite side to offset these small torque ratios (verification using mass). This procedure was repeated three times on each setting of the displacement sensor (repeatability) and performed two sets (reproducibility).

3.3 Result

Figure 7 shows the variation in torque ratio during displacement measurement obtained from the output of the torque transducers and small mass loading on the opposite side. The linear relationship between the double logarithmic scale of T (or W) and $\Delta T/T$ was reproduced during displacement measurement.

Figure 8 shows the results of displacement measurement. It is clear that both MBs were situated outside of the vertical position throughout the range from 5 N·m to 1 kN·m at 48 mm below the measurement axis. According to the torsional spring model, this means that the arm lengths are longer than the values measured by CMM and compensation factors for the nominal length of 500 mm become smaller than 1. The parameters were obtained from the torsional spring model as follows:

β = 91,6 N/rad,
C_A = 0,000014044,
$x_{0(R)}$ = 105,0 μm,
$x_{0(L)}$ = 78,9 μm,
$L_{0(R)}$' = 500,0197 mm and
$L_{0(L)}$' = 500,0126 mm.

Table I shows compensation factor C_L, which is concerned with load dependency calculated by

$$C_L = \frac{L_0}{L_0' + \frac{\beta}{W_i + \beta} x_0}, \quad (9)$$

where the arm length L_0' is expressed by the following equations (see Fig.3) according to the new definition from the model.

$$L_{0(R)}' = L_{u(R)} + x_{(R)} \quad \text{and} \quad (10a)$$

$$L_{0(L)}' = L_{u(L)} + x_{(L)} . \quad (10b)$$

If the calibration results obtained by the 1 kN·m-DWTSM in the ILC are compensated by these factors, the deviation becomes farther from the values of PTB, hence the torsional spring model is unfortunately not appropriate to explain the ILC deviations themselves. This model, however, may be generally useful for evaluating the arm length using MBs at the end of it.

4. ASYMMETRIC STRESS DISTRIBUTION MODEL

4.1 Principle

Another consideration for the load dependency may be attributed to the asymmetric stress distribution in the thickness direction of MBs. It was presumed that the asymmetric distribution was caused by the outward bend of MBs as shown in Fig.9. This drives the reference line inward, i.e., makes the effective arm length shorter than that in the case of no bend (the arm length obtained by CMM).

To verify this effect, another arm balancing test was conducted changing the MB thickness from 100 μm to 50 μm. Although this test gives only the relative value of the arm length between right and left sides and the difference of the reference lines in the case from 100 μm MB to 50 μm MB, the test makes the location range of the reference line narrower than the MB thickness. Thus, uncertainty of the arm length can be predicted more correctly.

The arm length L_0' is defined by (10a) and (10b) again in this model, where it is obvious that $x_{0(R)} > x_{0(L)}$ from the experiment results given in chapters 2 and 3.

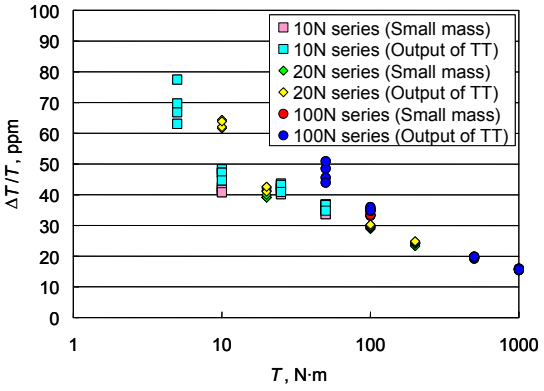

Fig. 7 Loading dependency of the torque ratio during displacement measurement

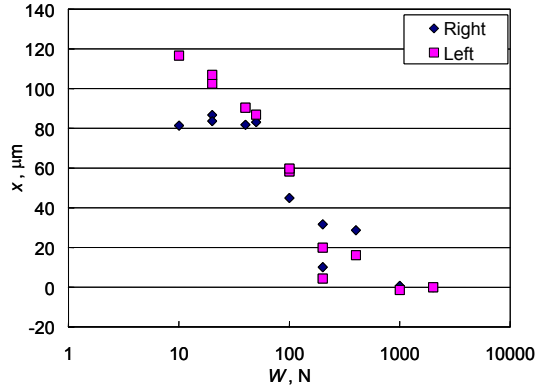

Fig. 8 Result of displacement measurement in the arm length direction

Table I Compensation factor C_L based on the torsional spring model

T, N·m	W, N	$L_{(R)}$, mm	$L_{(L)}$, mm	$C_{L(R)}$	$C_{L(L)}$
5	10	500,1143	500,0838	0,9998012	0,9998672
50	100	500,0699	500,0504	0,9998901	0,9999341
100	200	500,0526	500,0374	0,9999245	0,9999599
250	500	500,0359	500,0249	0,9999580	0,9999851
1000	2000	500,0243	500,0161	0,9999813	1,0000026
Infinity	Infinity	500,0197	500,0126	0,9999905	1,0000095

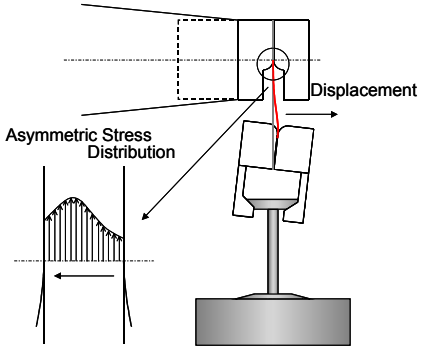

Fig. 9 Hypothesis of asymmetric stress distribution in MB

Table II Relative positions of reference lines when changing MB thickness

Exp.	MB thickness		Relative positions
	(L), μm	(R), μm	
A	100	100	$\delta x_{RL}\|_{100} = x_{(R)}\|_{100} - x_{(L)}\|_{100}$
B	100	50	$\delta x_{RL}\|_{50\text{-}100} = x_{(R)}\|_{50} - x_{(L)}\|_{100}$
C	50	100	$\delta x_{RL}\|_{100\text{-}50} = x_{(R)}\|_{100} - x_{(L)}\|_{50}$
D	50	50	$\delta x_{RL}\|_{50} = x_{(R)}\|_{50} - x_{(L)}\|_{50}$
			↓ $\delta x_{(R)}\|_{100\text{-}50} = x_{(R)}\|_{100} - x_{(R)}\|_{50}$ $\delta x_{(L)}\|_{100\text{-}50} = x_{(L)}\|_{100} - x_{(L)}\|_{50}$

The arm balancing tests of four patterns were conducted while changing the MB thickness for each side as shown in Table II. The symbols for relative positions are defined in Fig.10(a) and 10(b).

The relationship between the reference line position and torque ratio given by the arm balancing test is expressed as

$$\frac{\Delta T}{T} = \frac{(L_{u(R)} + x_{(R)}) \cdot W_i - (L_{u(L)} + x_{(L)}) \cdot W_i}{L \cdot W_i}$$

$$= C_A' + \frac{x_{(R)} - x_{(L)}}{L}, \qquad (11)$$

where

$$C_A' = \frac{L_{u(R)} - L_{u(L)}}{L}. \qquad (12)$$

Each relative position in Table II can be obtained by the experiments from A to D as follows:

$$\left.\frac{\Delta T}{T}\right|_A = C_A' + \frac{x_{(R)}|_{100} - x_{(L)}|_{100}}{L} = C_A' + \frac{\delta x_{RL}|_{100}}{L}, \qquad (13a)$$

$$\left.\frac{\Delta T}{T}\right|_B = C_A' + \frac{x_{(R)}|_{50} - x_{(L)}|_{100}}{L} = C_A' + \frac{\delta x_{RL}|_{50-100}}{L}, \qquad (13b)$$

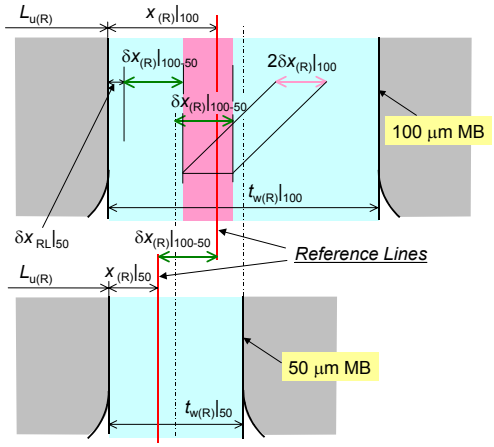

Fig.10(a) Definition of reference line position range for the right-side MB

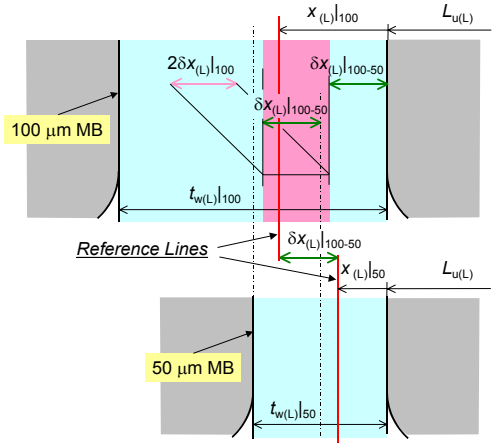

Fig.10(b) Definition of reference line position range for the left-side MB

$$\left.\frac{\Delta T}{T}\right|_C = C_A' + \frac{x_{(R)}|_{100} - x_{(L)}|_{50}}{L} = C_A' + \frac{\delta x_{RL}|_{100-50}}{L}, \qquad (13c)$$

$$\left.\frac{\Delta T}{T}\right|_D = C_A' + \frac{x_{(R)}|_{50} - x_{(L)}|_{50}}{L} = C_A' + \frac{\delta x_{RL}|_{50}}{L}. \qquad (13d)$$

The reference line positions and their regions are estimated by the following procedure:

(a) From the fact that $x_{(R)} > x_{(L)}$, $\delta x_{RL}|_{50}$ should be a positive value, hence the lower limit of the reference line position for the 100 μm MB on the right side can be determined as the sum of $\delta x_{RL}|_{50}$ and $\delta x_{(R)}|_{100\text{-}50}$.

(b) The upper limit can be expressed as the sum of $(t_{w(R)}|_{50})/2$ and $\delta x_{(R)}|_{100\text{-}50}$, because $x_{(R)}|_{50} \le (t_{w(R)}|_{50})/2$ is

true from the hypothesis of the inward biased stress distribution.

(c) Therefore, the shaded range in Fig.10(a) corresponds to the possible width of the reference line on the right side. Provided the range is the whole width of the rectangular distribution $2\delta x_{(R)}|_{100}$, the median value is simply the position of the reference line, i.e.:

$$\delta x_{(R)}\big|_{100} = \left(t_{w(R)}\big|_{50}\right)/4 - \delta x_{RL}\big|_{50}/2\,, \qquad (14)$$

$$x_{(R)}\big|_{100} = \delta x_{RL}\big|_{50} + \delta x_{(R)}\big|_{100-50} + \delta x_{(R)}\big|_{100}\,. \qquad (15)$$

(d) On the other hand, the lower limit of the reference line position for the 100 μm MB on the left side can be easily determined as $\delta x_{(L)}|_{100\text{-}50}$ itself.

(e) The upper limit can also be expressed as the sum of $(t_{w(L)}|_{50})/2$ and $\delta x_{(L)}|_{100\text{-}50}$ because $x_{(L)}|_{50} \le (t_{w(L)}|_{50})/2$ is true from the hypothesis of inward biased stress distribution.

(f) Therefore, the shaded range in Fig.10(b) corresponds to the possible width of the reference line on the left side.

(g) Provided this range is the whole width of the rectangular distribution $2\delta x_{(L)}|_{100}$, $\delta x_{(L)}|_{100}$ can be simply expressed as

$$\delta x_{(L)}\big|_{100} = (t_{w(L)}\big|_{50})/4\,. \qquad (16)$$

(h) $x_{(L)}|_{100}$ can be calculated from (11) and (15).

4.2 Experimental procedure

The arm balancing test was conducted using 100 N deadweight series, with equivalent torque step of 200, 400, 600, 800 and 1000 N·m. This loading was repeated three times for each experimental condition A, B, C, D and A again (see Table II), and the torque ratio was recorded from the output of the torque transducer of 100 N·m R.O.

4.3 Result

Figure 11 shows the measured torque ratio obtained by experiments A to D in Table II. It is obvious that the torque ratios saturate at certain values. Then, from the values at T = 1000 N·m, re-estimated values of arm length and the compensation factor at 20 °C when using 100 μm MB on both sides were calculated as follows:

$x_{(R)} = x_{(R)}|_{100} = 0{,}0410 \pm 0{,}0136$ mm,
$x_{(L)} = x_{(L)}|_{100} = 0{,}0315 \pm 0{,}0168$ mm,
$L_{0(R)}' = 500{,}0054 \pm 0{,}0292$ mm,
$L_{0(L)}' = 499{,}9984 \pm 0{,}0307$ mm,
$C_{L(R)} = 1{,}0000190$ and
$C_{L(L)} = 1{,}0000381$.

The measurement and calculation results are indicated in Table III for each length defined in Section 4.1 and related uncertainties obtained by the asymmetric stress distribution model. The measurement results of MB thickness themselves are also shown in Table III. The uncertainty ascribable to the deadweight load dependency of the arm lengths is expressed by $U_{load.lgt}$, combining the net torque deviations due to the load dependency (which is 51 ppm; see section 2.2) with the uncertainty of reference line position in MB $U(x|_{100})$.

The arm length could be re-evaluated more correctly. As a result of re-calculating the ILC deviation using the above new compensation factors, E_n number became less than 1 in almost throughout the torque range. However, cause of the ILC deviation is not completely clear. Other possible causes of the deviations are: stability of the torque transfer standards, cross-talking among the channels in the amplifier, problems with the power supply, and/or other unidentified reasons. The authors will continue investigating these issues for the future ILC.

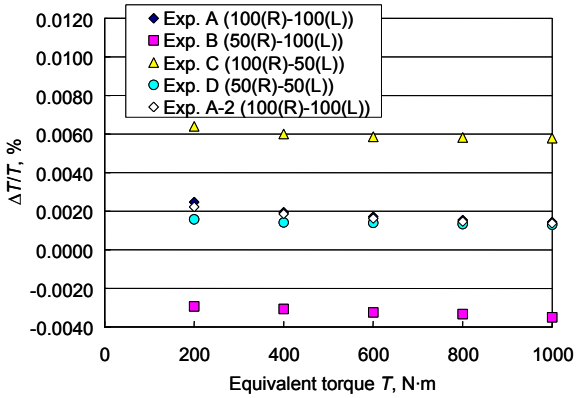

Fig.11 Measurement result of torque ratios with changing MB thickness

Table III Each length in MB and related uncertainties obtained by the asymmetric stress distribution model

Lengths			
$t_{w(L)}\|_{100}$, μm	101,0	$t_{w(R)}\|_{100}$, μm	100,9
$t_{w(L)}\|_{50}$, μm	47,8	$t_{w(R)}\|_{50}$, μm	52,0
		$\delta x_{RL}\|_{50}$, μm	8,9
$\delta x_{(L)}\|_{100\text{-}50}$, μm	22,9	$\delta x_{(R)}\|_{100\text{-}50}$, μm	23,5
$\delta x_{(L)}\|_{100}$, μm	12,0	$\delta x_{(R)}\|_{100}$, μm	8,6
$x_{(L)}\|_{100}$, μm	31,5	$x_{(R)}\|_{100}$, μm	41,0
Uncertainties (k = 2)			
$u(t_{w(L)}\|_{50})$, μm	4,3	$u(t_{w(R)}\|_{50})$, μm	4,3
$u(\delta x_{(L)}\|_{100\text{-}50})$, μm	2,0	$u(\delta x_{(R)}\|_{100\text{-}50})$, μm	2,0
$u(\delta x_{(L)}\|_{100})$, μm	6,9	$u(\delta x_{(R)}\|_{100})$, μm	4,9
$u(x_{(L)}\|_{100})$, μm	8,4	$u(x_{(R)}\|_{100})$, μm	6,8
$U(x_{(L)}\|_{100})$, ppm	33,5	$U(x_{(R)}\|_{100})$, ppm	27,3
$U_{load.lgt(L)}$, ppm	61,0	$U_{load.lgt(R)}$, ppm	57,8

5. IMPROVEMENT OF UNCERTAINTY IN THE TORQUE STANDARD MACHINE

Finally, in order to improve the load dependency of the arm length, additional initial weights were mounted on the hanger parts just below the MB as shown in Fig.12. The mass of the weights is about 7,6 kg for each side. The same experiment was carried out as described in chapter 2, in which the 100 μm MBs were used for the loading point at the ends of the arm.

The initial weights reduced the movement of the reference line by applying pre-tension on the MBs as shown in Fig.13. The maximum $\Delta T/T$ became within 24 ppm in the range from 5 N·m to 1 kN·m. Improved arm lengths are as follows:

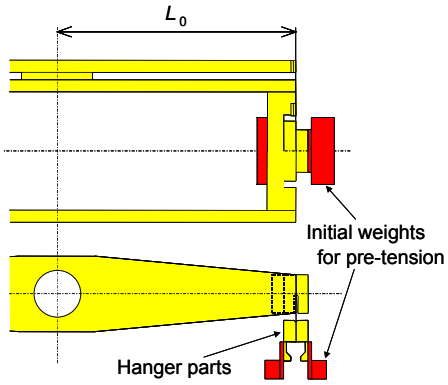

Fig.12 Additional initial weights

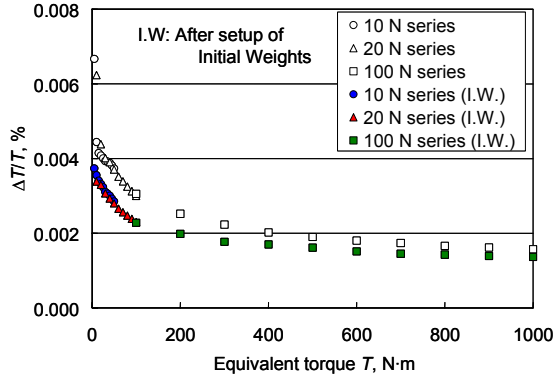

Fig.13 Improvement in load dependency of the arm length

Table IV Uncertainty budget table for the torque standard machine of NMIJ

Uncertainty contributions (relative)		ppm
Mass of linkage weights	u_{mass}	2,5
Local acceleration of gravity	u_{grav}	0,23
Influence of air buoyancy on the deadweight loading	u_{buoy}	2,5
Initial moment-arm length (including CMM measurement, temperature compensation)	u_{act_lgt}	6,0
Influence of the variation in the reference line due to deadweight loading on the arm length	u_{load_lgt}	**31 → 21**
Influence of the flexure in the arm due to deadweight loading on the arm length	u_{flx_lgt}	2,1
Sensitivity reciprocal of the fulcrum (aerostatic bearing)	u_{sr}	10
Reproducibility of the sensitivity in the fulcrum	u_{ssv}	2,0
Relative combined standard uncertainty	u_{c_tsm}	24
Relative expanded uncertainty (k=2)	U_{tsm}	49

$L_{0(R)}$' = 500,0054 ± 0,0185 mm and
$L_{0(L)}$' = 499,9984 ± 0,0212 mm.

Table IV shows the uncertainty budget of the 1 kN·m-DWTSM of NMIJ. The total expanded relative uncertainty was re-evaluated as 49 ppm due to the improvement of the load dependency of the arm length.

6. CONCLUSIONS

The authors re-verified the moment-arm length in order to attempt to explain the deviations that occurred in the ILC of torque between PTB and NMIJ. The following conclusions were drawn.

(1) Load dependency existed. The maximum relative torque deviation was +67 ppm (net variation was +51 ppm). The arm ratio of +16 ppm was different from the values obtained by CMM measurement (-5 ppm).

(2) As results of the arm balancing test while changing the MB thickness from 100 μm to 50 μm and applying the asymmetric stress distribution model, the arm length could be re-evaluated more correctly. However, the compensation result using these values was not sufficient to explain the ILC deviations.

(3) The use of additional weights to apply pre-tension on the MBs could be effective, reducing the load dependency of the arm length from +51 ppm to +24 ppm.

REFERENCES

[1] D.Peschel, T.Bruns, Z.Zhang, W.Shang and K.Ohgushi, "International Loop Comparison of the Torque Standard Machines, Part 3, PTB/Germany - NMIJ/AIST/Japan", PTB-Bericht, MA-70, in press.

[2] D.Roeske, "Realization of the Unit of Torque - Determination of the Force - Acting Line Position in Thin Metal Belts", Proc. 15th IMEKO TC-3 Conference, pp.261-264, Madrid, Spain, Oct., 1996.

[3] K.Ohgushi, T.Tojo and E.Furuta, "Development of the 1 kN·m Torque Standard Machine", Proc. XVI IMEKO World Conference, pp.217-223, Vienna, Austria, Sept., 2000.

Authors:

Koji Ohgushi, Researcher, Mass and Force Stds. Sect., National Metrology Institute of Japan, AIST Central 3, 1-1-1 Umezono, Tsukuba, 305-8563, Japan. Tel: +81-298-61-4012, Fax: +81-29-861-4399, E-mail: k.ohgushi@aist.go.jp.

Takashi Ota, Technician, Mass and Force Stds. Sect., National Metrology Institute of Japan, Tel: +81-29-861-4153, Fax: +81-298-61-4399, E-mail: t-ota@aist.go.jp.

Kazunaga Ueda, Chief, Mass and Force Stds. Sect., National Metrology Institute of Japan, Tel: +81-29-861-4153, Fax: +81-298-61-4399, E-mail: kazunaga-ueda@aist.go.jp.

Diedert Peschel, Head, Torque Section, Physikalisch-Technische Bundesanstalt, Bundesallee 100, 38116 Braunschweig, Germany. Tel: +49-531-592-1130, Fax: +49-531-592-1105, E-mail: diedert.peschel@ptb.de.

Thomas Bruns, Researcher, Torque Section, Physikalisch-Technische Bundesanstalt, Tel: +49-531-592-1132, Fax: +49-531-592-1105, E-mail: thomas.bruns@ptb.de.